Scorpion-Lift Ant-Weight BattleBot

ECE 445 Final Report — Spring 2026

Chen Meng (meng28)

Zisu Jiang (zisuj2)

Zixin Mao (zixinm2)

Professor: Victor Gruev

TA: Zhuoer Zhang

Project No. 4

May 2026

Abstract

Scorpion-Lift is an ant-weight BattleBot designed to improve mobility, lifting ability, and stability during combat. The system uses a tracked differential-drive base for traction, dual high-torque servo arms for opponent lifting, a rear tail stinger for anti-tip support, ESP32-based Wi-Fi control, and a dedicated power architecture for motors and servos. Verification results showed that the robot achieved an average straight-line speed of 0.706 m/s and completed full-differential turning without tread derailment. The lifting arms raised a 2 lb load by at least 30 mm in 0.76 s. The tail resisted a 5.0 N front lifting force with a maximum pitch angle of 31° and deployed in 0.76 s. Wireless control remained stable at 10 m, and the failsafe stopped outputs within 580 ms. The system operated continuously for a 2-minute match test without shutdown or brownout.

Table of Contents

* Note that the verifications are included in the subsystem design sections.

1. Introduction

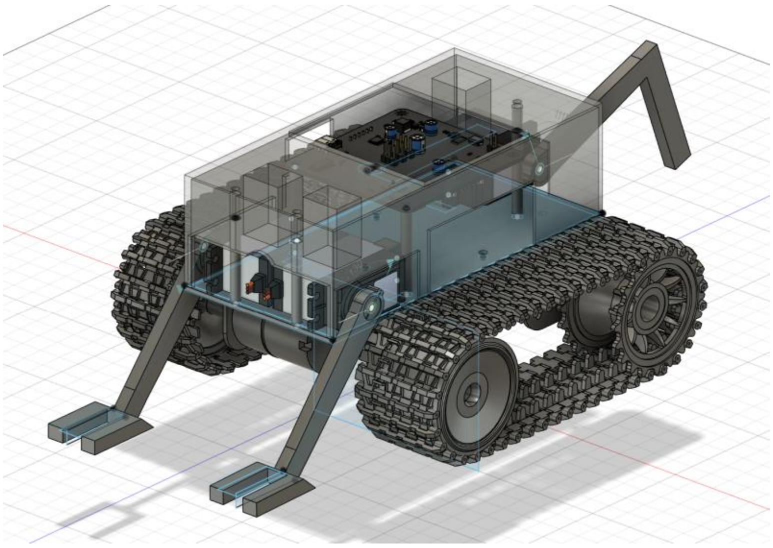

Figure 1: 3D Model of the Scorpion-Lift Battlebot

1.1 Problem and Solution

Scorpion-Lift is an antweight BattleBot designed for the small combat-robot setting [1] and addresses two common failure modes in such robots: traction loss during pushing and backward tipping during lifting [2]. The primary goal of the project was to engineer a robot that can maintain stable tracked mobility, effectively lift or control an opponent from the front, and resist backward rotation utilizing a rear tail brace.

To ensure the proposed solution was robust, several block-level design changes were implemented during development to mitigate integration risks and enhance overall reliability. To address mobility vulnerabilities, the track geometry was transitioned to a caterpillar-style continuous track layout. To minimize mechanical backlash and binding, the lifting arm subsystem was simplified from a four-bar linkage to a direct claw linkage. Furthermore, the tail subsystem was updated from a separate motor-driver-based actuator to a DS3218 servo-driven stinger arm. Finally, to streamline operations, the wireless subsystem was shifted from Bluetooth control to a Wi-Fi webpage interface, allowing control and telemetry to be seamlessly combined. These iterative solutions significantly improved mechanical reliability, simplified system control, and ensured the final robot could successfully meet its core performance requirements

1.2 Functionality

The Scorpion-Lift system is divided into five major functional subsystems: tracked mobility and drive, dual lifting arms, scorpion tail stinger, wireless control, and power, safety, and compliance. The power subsystem distributes energy from an 11.1 V lithium polymer battery to the motor drivers, a 5 V servo rail, and a 3.3 V logic rail. The wireless control subsystem utilizes an ESP32-WROOM module to receive Wi-Fi commands and distribute pulse-width modulation control signals to the drive motors, lifting arms, and tail servo. For physical actuation, the drive subsystem utilizes two MG310 gearmotors, coupled with continuous tracks, for both translational and rotational motion. The lifting subsystem employs two DS3218 servos driving direct claw linkages to elevate loads, while the tail subsystem uses an additional DS3218 servo to deploy the rear stinger arm for anti-tip support.

The functionality of the complete system is verified against a strict set of performance requirements evaluating mobility, opponent control, stability, wireless reliability, and safety. Functionally, the robot must achieve a straight-line speed of at least 0.5 m/s under full system load, complete five consecutive full-differential turns without tread derailment, and sustain continuous operation during a 2-minute match. The lifting arms are required to elevate a 2 lb test load by at least 30 mm within 3 s. For stability, the deployed tail must successfully resist backward tipping when a 5.0 N upward force is applied at the front of the chassis. Finally, the wireless functionality requires maintaining a stable Wi-Fi connection at a 10 m line-of-sight and features a safety failsafe designed to disable all motor and actuator outputs within 800 ms of signal loss.

2. Design

2.1 Hardware Design

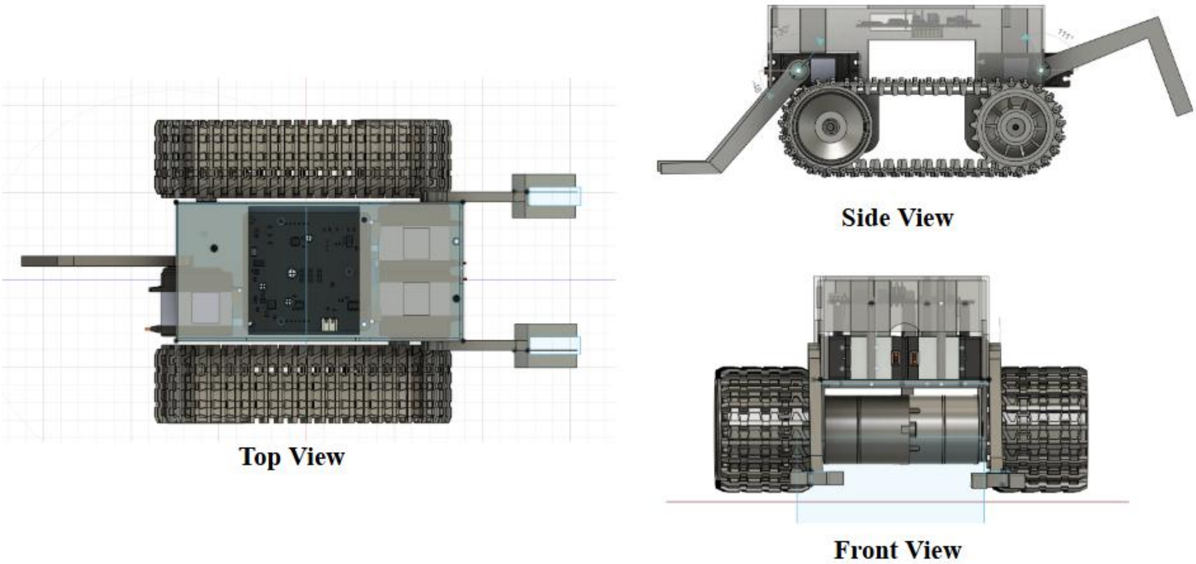

Figure 2: 3-View Diagram of the Hardware Model

The physical and electrical layout of our battlebot is designed to prioritize robust mobility, chassis stability, and effective opponent manipulation. By maximizing our traction and preventing backward tipping during offensive maneuvers, we have constructed a highly stable platform. Our battlebot employs protective safety measures and structural optimizations to maintain durability during combat. For instance, to prevent mechanical failure under the high torque required for lifting large weights, we reduced the inner diameter of the spline hole in the CAD model by 0.05 mm, which prevents the slotted press-fit connections from stripping. Furthermore, the chassis incorporates extra under-board space to safely house the battery.

Within combat robotics, maintaining control of the opponent is essential. We opted for a lifter weapon system utilizing dual lifting arms. While initially considering a 4-bar linkage mechanism, we ultimately pivoted to a direct claw linkage. The direct claw configuration features fewer joints than a 4-bar linkage, making the mechanism stiffer and significantly more reliable. This reduction in mechanical complexity also ensures there is less backlash and binding when the arms are placed under heavy loads.

For our drivetrain, we focused on eliminating common failure points such as traction loss and tread derailment. Initially, our original design utilized a crown-pulley geometry. While this geometry is theoretically effective for keeping belts aligned, further evaluation revealed that the track belt associated with the crown-pulley wheels was far too thin. This thin profile presented a potential critical weakness in the highly destructive and intense environment of combat robotics. Consequently, we iterated upon this structure and transitioned to a plastic caterpillar continuous track design. This finalized continuous track system significantly enhances the defensive durability and impact resistance of the mobility platform while maintaining reliable traction. To complement the front lifting claws and prevent the chassis from tipping backward during lifts, we incorporated a rear scorpion tail brace.

2.2 Block Diagram

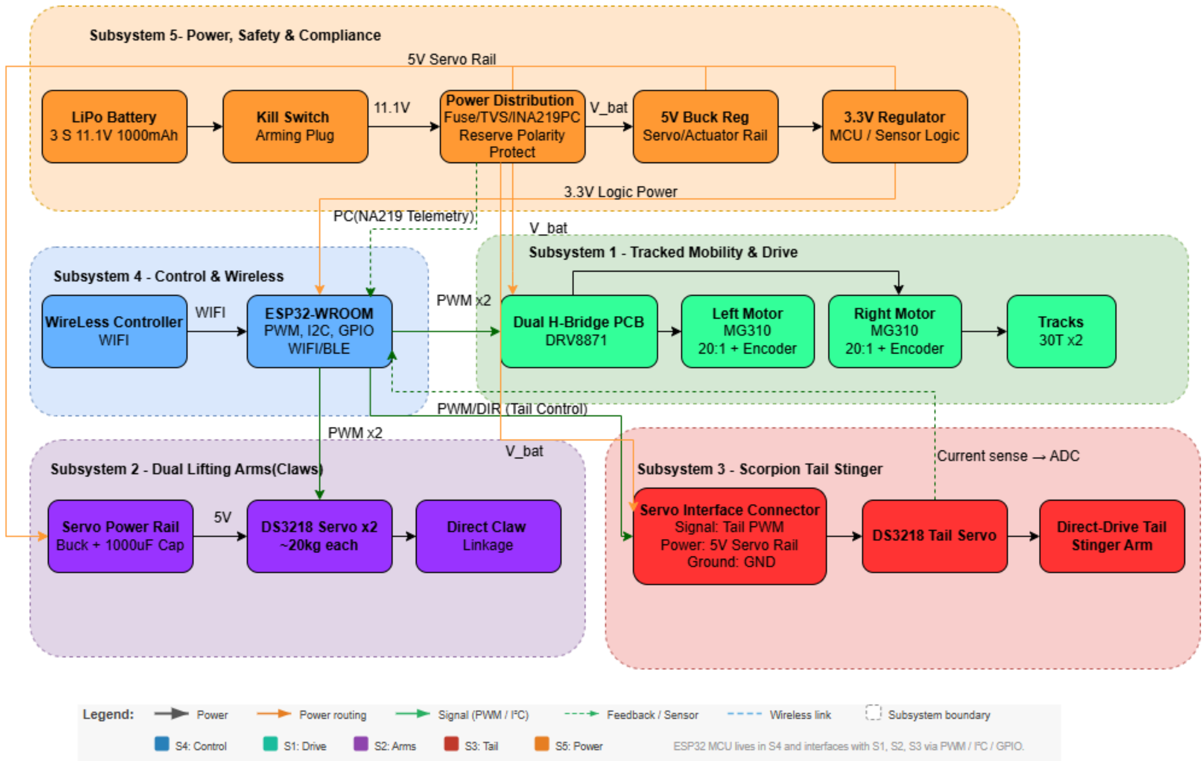

Figure 3: Overall Block Diagram

This block diagram shows the full system architecture of the Scorpion-Lift BattleBot. The robot is divided into five main subsystems: power, tracked mobility, lifting arms, tail stinger, and wireless control. The LiPo battery first passes through a kill switch and power distribution stage, then supplies regulated 5 V power for the servos and 3.3 V power for the ESP32 controller and sensors. The ESP32 handles Wi-Fi control, sends PWM signals to the drive motors, lifting arm servos, and tail servo, and receives telemetry feedback such as battery voltage and current sensing. The tracked mobility subsystem uses a dual H-bridge driver to control the left and right MG310 motors, which drive the continuous tracks. The dual lifting arms use two DS3218 servos connected to direct claw linkages, while the rear tail stinger uses another DS3218 servo to deploy the stabilizing tail arm. Overall, the diagram shows how power, control signals, and feedback paths connect all subsystems into one integrated robot system.

2.3 Subsystem Design

2.3.1 Tracked Mobility Subsystem

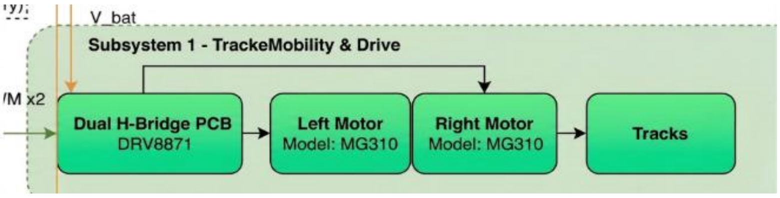

Figure 4: Block Diagram of Subsystem 1

Design Procedure

The tracked mobility and drive subsystem provides all translational and rotational motion for the Scorpion-Lift battlebot. During component selection, commercial 100:1 metal gearmotor options were also reviewed [4], and commercial track-set form factors informed the early mobility concept [8]. The subsystem uses two MG310 direct current (DC) gearmotors, a custom dual H-bridge printed circuit board (PCB) featuring the DRV8871 driver, and a plastic caterpillar continuous track system.

The original design considered utilizing the DRV8701 external H-bridge driver for the motor control. This approach could provide extreme current capacities exceeding 50 A, but it required four discrete external N-channel MOSFETs, which significantly increased the PCB footprint and design complexity. Because the battlebot's peak current is approximately 2.6 A, this component was heavily over-engineered. The final design, therefore, used the DRV8871 integrated H-bridge driver. This design features MOSFETs built inside the package, reducing design complexity while easily meeting the 3.6 A peak current requirement without unnecessary bulk.

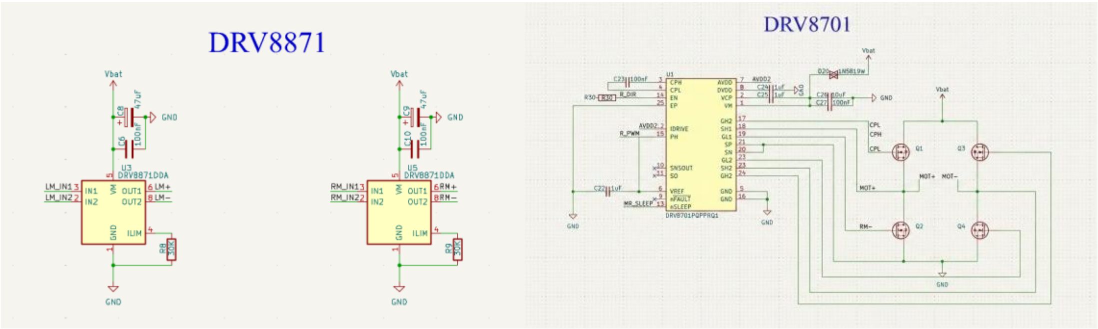

Figure 5: Contrast Between DRV8871 and DRV8701 PCB Interface

The actuator selection was also based on durability and thermal resistance during the fabrication process. The initial design utilized N20 DC motors. However, the N20 motors feature fragile copper leaf pins that are unstable, and their plastic end caps are susceptible to thermal deformation when soldering. The MG310 DC motor was selected instead because it provides robust metal solder tips and a heat-resistant terminal assembly. Furthermore, the original track design utilized a crown-pulley geometry to passively self-center the treads. During evaluation, it became apparent that the flat track belt associated with this geometry was too thin and presented a critical weakness for intense combat. The final design pivoted to a plastic caterpillar continuous track, which significantly enhances the defensive durability and impact resistance of the mobility platform.

Figure 6: MG310 DC Motor

Design Details

The final mobility assembly uses two MG310 DC gearmotors mounted on the left and right sides of the chassis. Each motor is driven by the DRV8871 dual H-bridge PCB, which is powered directly from the main battery voltage rail. The motors are mechanically coupled to the rear drive sprockets of the plastic caterpillar continuous track system. This differential-drive configuration allows the robot to achieve rapid straight-line speeds while maintaining the ability to perform zero-radius turns. The track system's durable plastic construction ensures that the treads remain securely on the sprockets even when subjected to lateral impact forces from opposing robots.

Verification

The main requirements for Subsystem 1 were that the drive system achieves a straight-line speed of at least 0.5 m/s under full system load and that the tracks prevent tread derailment during full-differential zero-radius turns. To verify the speed requirement, the robot was driven over a testing distance of 2.47 m on a flat surface at full throttle, and the time was recorded using a stopwatch across three trials. To verify the track retention requirement, the robot was commanded to execute five consecutive full-differential turns, alternating left and right for 3 seconds in each direction, followed by visual inspection. The subsystem passed if the average speed exceeded 0.5 m/s and no derailment occurred.

2.3.2 Dual Lifting Arms Subsystem

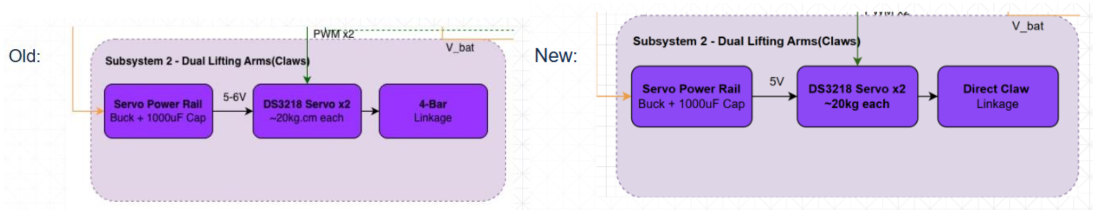

Figure 7: Block Diagram of Subsystem 2

Design Procedure

Subsystem 2 provides the lifting function for Scorpion-Lift. The subsystem uses two DS3218 metal-gear servos [5], a direct claw linkage, polylactic acid plus (PLA+) structural arms, a dedicated 5 V servo rail, and a 1000 µF bulk capacitor. The arms are controlled by pulse-width modulation (PWM) signals from the ESP32 controller. **Figure 8** shows the final dual-arm mechanism and its connection to the servo power rail.

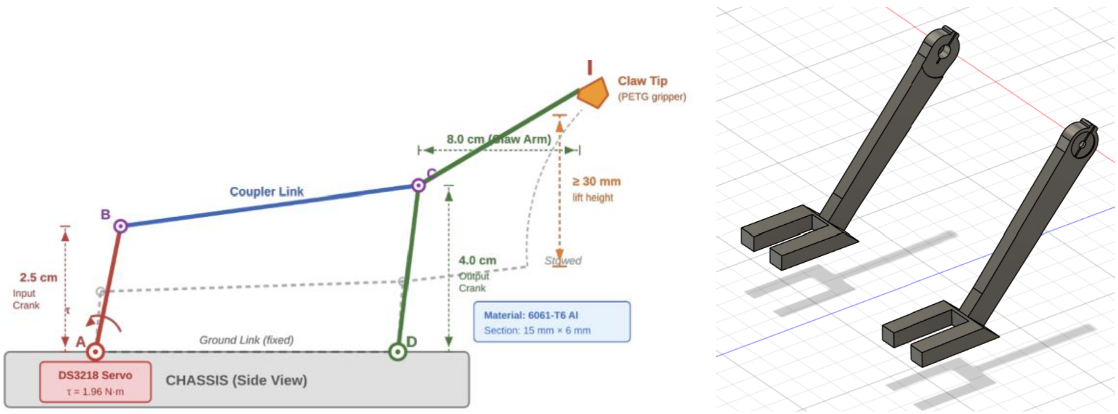

Figure 8: Previous Front Claw Model and Current 3D Model

The original design used a four-bar linkage between the servo and claw. Although it could provide more controlled motion, it added joints, tolerance sensitivity, and possible backlash or binding. The final design used a direct claw linkage because it has fewer moving parts, a stiffer load path, and simpler assembly. This made it more reliable for lifting inside the small ant-weight chassis.

The actuator was selected based on torque margin and control simplicity. A low-torque servo did not provide enough lifting margin, while a DC motor with a gearbox required extra feedback and control. The DS3218 servo was chosen because it provides about 20 kg·cm of torque, built-in position control, metal gears, and direct PWM compatibility with the ESP32. Its higher current draw was handled using a separate 5 V rail and a 1000 µF capacitor.

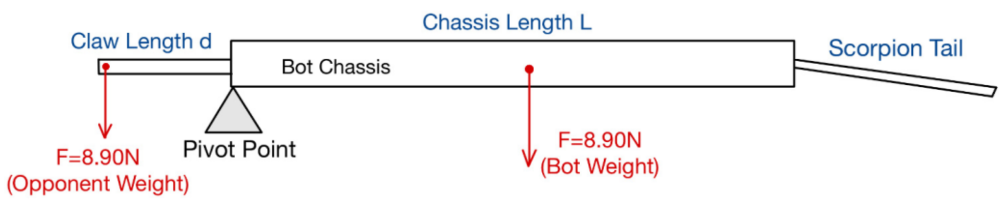

Figure 9: Force Analysis with Pivot Point at the Front

The lifting torque requirement was estimated using the load force and the distance from the servo axis to the load point:

$\tau\_load = F\_load \times L\_claw$

For a 2 lb load, the equivalent force is:

$F\_load = 2 \text{ lbf} \times 4.448 \text{ N/lbf} = 8.90 \text{ N}$

Using an approximate claw moment arm of 60 mm from the CAD model, the required lifting torque is:

$\tau\_load = 8.90 \text{ N} \times 0.060 \text{ m} = 0.534 \text{ N·m}$

The nominal DS3218 servo torque is:

$\tau\_servo = 20 \text{ kg·cm} \times 9.81 \text{ N/kg} \times 0.01 \text{ m/cm} = 1.96 \text{ N·m}$

Therefore, the approximate torque safety factor is:

$\text{Safety Factor} = \tau\_servo / \tau\_load = 1.96 / 0.534 = 3.67$

This provides a torque margin of approximately 3.7 if one servo carries the full 2 lb load. Since the final design uses two arms together, the practical margin is higher when the load is shared between the two servos. This margin was important because the real mechanism includes friction, print tolerance, impact loading, and voltage sag during servo startup.

Design Details

The final arm assembly uses two DS3218 servos mounted near the front of the chassis, with each servo driving one direct claw link. The PLA+ printed links provide a lightweight structure while staying stiff enough for the lifting requirement. The servo power rail is separated from the ESP32 logic rail to reduce the effect of servo current spikes on the microcontroller. During testing, the first printed arms slipped at the servo spline because the spline holes were slightly oversized. To fix this, the CAD spline hole diameter was reduced by 0.05 mm, and the reprinted arms transferred torque reliably under load.

Verification

The main requirement for Subsystem 2 was to lift a 2 lb load by at least 30 mm within 3 s. For verification, the load was placed on the claw tip, the ESP32 sent the lift command, and the height and time were measured using a ruler and stopwatch. The arms lifted the load by at least 30 mm in 0.76 s, which was well below the 3 s limit. Therefore, the final arm design satisfied the lifting requirement with a large time margin. The main uncertainty was the spline fit, but this issue was resolved by tightening the CAD tolerance and reprinting the arms.

2.3.3 Scorpion Tail Stinger Subsystem

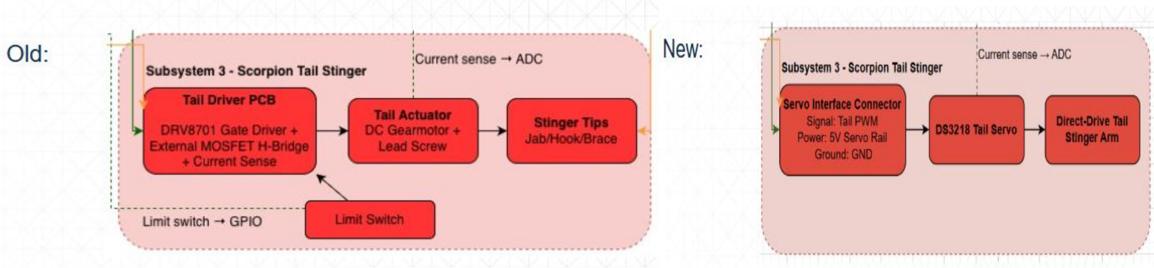

Figure 10: Block Diagrams of Subsystem 3

Design Procedure

Subsystem 3 provides rear stability during lifting and prevents the robot from tipping backward when an opponent applies an upward force at the front. The subsystem uses one DS3218 high-torque servo, a direct-drive PLA+ tail stinger arm, a 5 V servo power rail, and a servo interface connector. The tail receives a PWM control signal from the ESP32 and deploys behind the rear of the chassis to create a bracing contact point with the ground. **Figures 10 through 12** shows the final tail stinger mechanism.

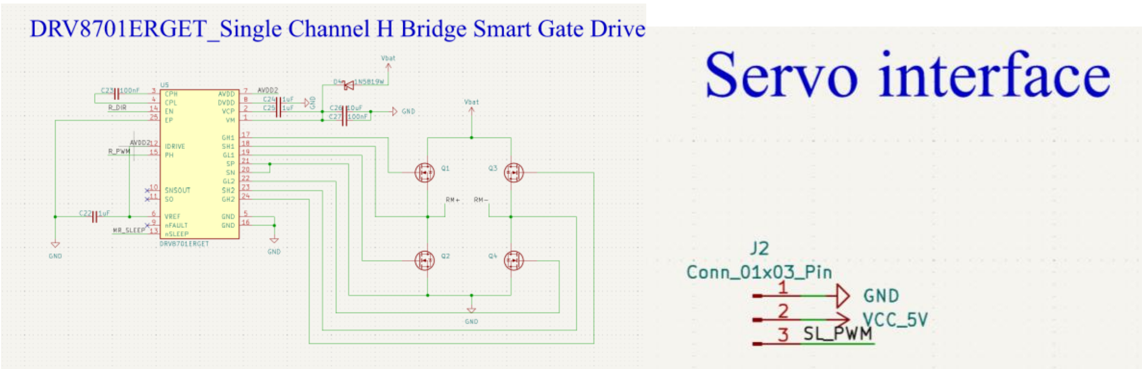

Figure 11: PCB Schematic of the DRV8701 Motor Driver and the DS3218 Servo Interface

The original tail design used a DRV8701-based PCB with an external MOSFET H-bridge to drive a DC actuator based on a 50:1 metal gearmotor [9]. However, this added electrical complexity, integration risk, and debugging time. Since the tail only needed to move between stowed and bracing positions, the final design replaced the H-bridge actuator with a DS3218 servo. This simplified control through PWM and reduced the number of power electronics components. The team also replaced multiple jab, hook, and brace tip options with one direct-drive tail stinger arm. This design reduced mechanical complexity and provided a more stable ground-contact point for preventing backward tipping.

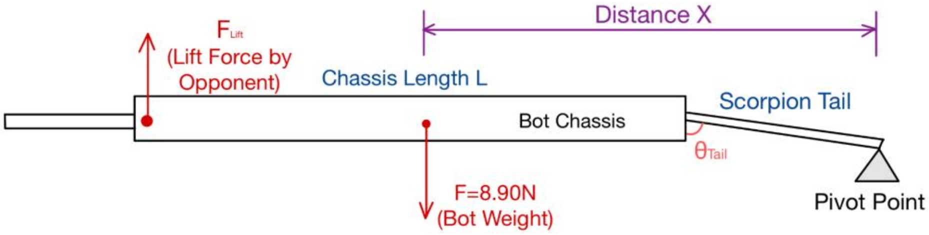

Figure 12: Force Analysis with Pivot Point at the Tail Tip

The anti-tip function was modeled using a static moment balance about the rear track contact point.

$$F_{tail} \times d_{tail} + W_{robot} \times d_{CG} \geq F_{front} \times d_{front}$$

Here, F_tail is the vertical reaction force from the tail, d_tail is the tail contact distance behind the rear track, W_robot is the robot's weight, d_CG is the center-of-gravity distance from the rear track, F_front is the upward force applied at the front, and d_front is the front lifting distance. This relationship shows that the deployed tail creates an additional stabilizing moment behind the robot, helping resist the front lifting moment and reducing the chance of backward tipping.

Design Details

The final tail subsystem uses a DS3218 servo mounted near the rear of the chassis. The tail stinger arm is directly connected to the servo shaft and moves from the stowed position to the bracing position through an ESP32 PWM command. The servo connector carries the PWM signal, 5 V power, and ground, and the tail shares the dedicated 5 V servo rail with the lifting arms. During testing, the original PLA+ tail tip slipped because of low floor friction, reducing its stabilizing effect. Double-sided tape was added to the tip, increasing friction and improving bracing consistency.

Verification

Subsystem 3 had two requirements: prevent backward tipping during front lifting and deploy from stowed to bracing position within 1.0 s. For the anti-tip test, the robot was placed on a flat surface with the tail deployed. A spring scale applied a 5.0 N upward force at the front center of the chassis for 5 s. The test passed if the pitch angle stayed below 45° and no full tip-over occurred. For the speed test, the ESP32 commanded full tail deployment, and the motion time was measured with a phone stopwatch. The test passed if deployment finished within 1.0 s.

2.3.4 Wireless Control Subsystem

Design Procedure

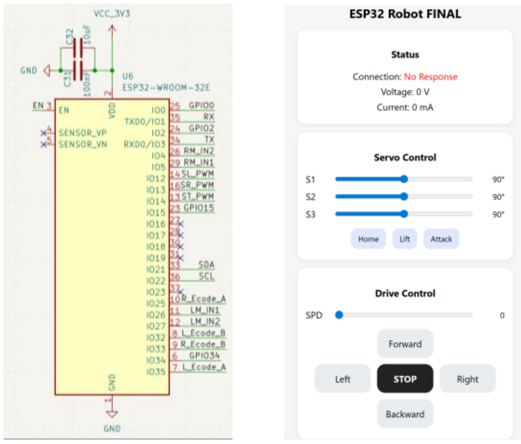

Figure 13: ESP32 pin-assignment schematic and webpage control interface for Subsystem 4.

Subsystem 4 uses the ESP32 as the main control and communication unit [6]. As shown in **Figure 13**, the ESP32 provides WiFi communication, PWM output, GPIO control, and I²C communication in one controller. This allowed the final design to control two drive motors, two lifting arm servos, one tail servo, and the INA219 telemetry monitor without adding a separate communication board.

The original design considered Bluetooth control, but the final implementation used a WiFi webpage interface. This interface simplified testing because the operator could send drive and servo commands while viewing voltage and current telemetry on the same page. A heartbeat failsafe was added to reduce the risk of continued motion after communication loss. The final firmware flow is shown in **Figure 14**.

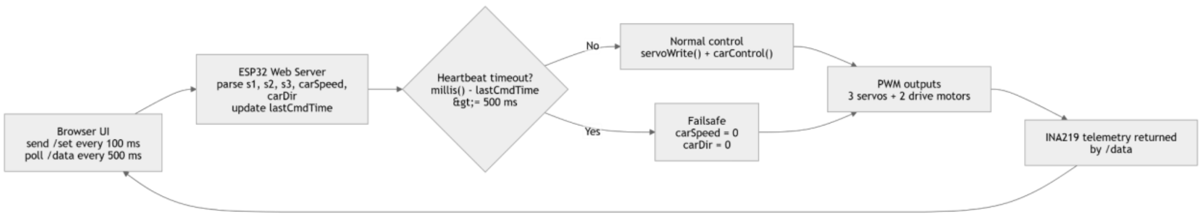

Figure 14: Wireless control and failsafe flowchart for the final ESP32 firmware.

Design Details

The ESP32 generates PWM signals for the drivetrain and three servos. The webpage sends updated control commands every 100 ms, and the ESP32 returns telemetry data every 500 ms. Servo PWM is generated at 50 Hz, while motor PWM is generated at 1 kHz for differential drive control.

The firmware records the time of the most recent valid command. If no command is received for 500 ms, the drive speed and direction are set to zero. This allows the ESP32 to function as the webpage host, actuator controller, telemetry interface, and safety monitor within one firmware structure.

Verification

The wireless link was tested at a 10 m line of sight distance, and the robot maintained stable WiFi control without noticeable command loss. The failsafe was tested by interrupting command transmission during operation. The drive outputs stopped after 580 ms, which satisfies the 800 ms requirement. Detailed results are listed in Appendix A.

2.3.5 Power, Safety, and Compliance Subsystem

Design Procedure

Subsystem 5 provides battery power distribution, voltage regulation, telemetry, and protection for the robot. As shown in **Figure 15**, the final design uses a 5 V rail for the servos and actuator side electronics and a 3.3 V rail for the ESP32 and sensors. Separate rails were used because servo current transients could otherwise disturb the controller supply.

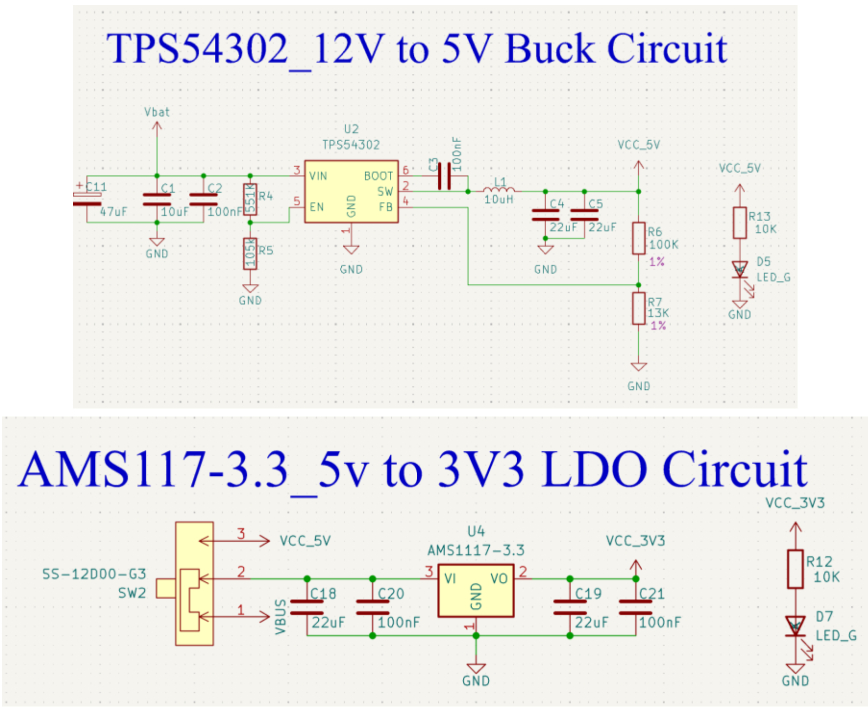

Figure 15: Subsystem 5 power regulation circuits, including the TPS54302 buck converter for the 5 V rail and the AMS1117-3.3 LDO regulator for the 3.3 V logic rail.

The robot is powered by a 3S LiPo battery. **Figure 17** shows the main battery path, including the arming plug, fuse, TVS protection, reverse polarity protection, and INA219 monitoring before the V_bat rail. A 1000 µF capacitor was added to the 5 V servo rail to reduce voltage droop during servo startup and simultaneous arm motion. The INA219 circuit in **Figure 16** provides battery current and voltage telemetry to the ESP32 over I²C [7].

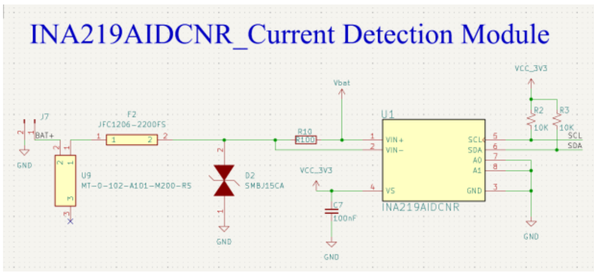

Figure 16: INA219 current and voltage monitoring circuit for Subsystem 5, which reports battery telemetry to the ESP32 over I²C.

Design Details

The final robot uses an 11.1 V, 1000 mAh 3S LiPo battery. Battery power first passes through the safety disconnect and protection stages shown in **Figure 17**. The protected V_bat rail supplies the drivetrain and the voltage regulation circuits.

The TPS54302 buck converter generates the 5 V rail, and the AMS1117-3.3 regulator derives the 3.3 V logic rail from the 5 V rail, as shown in **Figure 15**. The INA219 monitor is placed on the main power path and communicates with the ESP32 over I²C, as shown in **Figure 16**. During final testing, USB power was used only for programming, while battery power was used for full load validation.

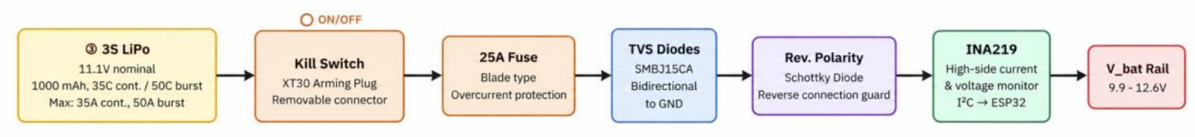

Figure 17: Main battery power distribution and protection path for Subsystem 5, from the 3S LiPo battery to the monitored V_bat rail.

Verification

The power subsystem was tested under simultaneous drive and servo operation. The INA219 measured a peak battery current of 2601 mA, and no ESP32 reset, shutdown, or brownout was observed. The robot also completed a 2-minute active load test with no communication loss or power interruption. These results indicate that the battery and regulated rail structure were sufficient for the final prototype. Detailed results are listed in Appendix A.

3. Costs

3.1 Parts

Part Category	Components Included	Vendor	Original Cost	Cost Paid (USD)
Amazon	SG90, INA219, AMS1117, ESP32, LM2596 buck modules	Amazon	$52.94	$52.94
Mechanical and actuation parts	Tracked chassis parts, MG310 gearmotors, DS3218 servos, battery pack, wheels, bearings, track links, assembly tools	Taobao	¥669.45	$98.28
PCB electronic components	DRV8871 drivers, INA219 ICs, AMS1117 regulators, TPS54302 or TPS54331 ICs, switches, fuses, capacitors, resistors, headers, USB C connectors, protection parts	Taobao	¥293.54	$43.09
Custom PCB prototypes	Three PCB design revisions	PCBWay	Course budget	$0.00
3D-printed parts	Chassis, lifting arms, direct claw links, tail stinger parts printed in 2070	Bambu Lab	Free	$0.00
Total				**$194.31**

Table 6: Table of Cost of Parts Used in the Project

3.2 Labor

Labor cost was estimated using the standard ECE 445 formula based on an hourly rate of **$42.50** and a multiplier of **2.5**. Assuming **60 hours** of work per team member, the labor cost was **$6,375** per person. For a three member team, the total estimated labor cost was **$19,125**.

4. Conclusion

4.1 Accomplishments

The Scorpion-Lift project successfully met its core objective of designing an antweight battle bot capable of overcoming common combat robotics failures, specifically traction loss and backward tipping. Through iterative engineering, the team successfully integrated mechanical, electrical, and firmware subsystems into a cohesive and functional prototype.

Key accomplishments include:

- **Tracked Mobility:** We successfully implemented a continuous caterpillar track system that achieved an average straight-line speed of 0.706 m/s, exceeding the 0.5 m/s requirement. The system also successfully completed zero-radius differential turns without any tread derailment.
- **Dual Lifting Arms:** The direct claw linkage effectively elevated a 2 lb opponent test load by at least 30 mm in just 0.76 seconds.
- **Scorpion Tail Stinger:** The servo-actuated tail successfully provided anti-tip support, deploying in 0.76 seconds. It resisted up to 5.5 N of front lifting force while maintaining a maximum chassis pitch angle of 31°, well below the 45° failure threshold.
- **Wireless Control and Safety:** We successfully developed a stable Wi-Fi-based control interface that maintained a reliable connection at a 10 m line-of-sight. Additionally, the implemented heartbeat failsafe successfully disabled all motor outputs within 580 ms of signal loss.
- **Power Reliability:** The custom power distribution system sustained continuous operation during a 2-minute simulated match and safely handled peak battery currents of 2601 mA without controller resets or brownouts.

4.2 Engineering Standards

The following standards apply to this project:

- IPC-2221B (Generic Standard on Printed Board Design) [3]: All custom PCBs will be designed with appropriate trace widths for current-carrying capacity, creepage and clearance distances for the 12 V power rail, and thermal relief pads for power components.
- UL 1642 (Lithium Batteries): The LiPo battery usage follows standard safety practices, including charge control, over-discharge protection, and current limiting.

- FCC Part 15 (Unintentional Radiators): The ESP32 module is FCC-certified. The custom PCB design will minimize EMI through proper grounding and decoupling.
- ANSI/UL 1244 (Electrical and Electronic Measuring and Testing Equipment): All test equipment used during verification will be calibrated and operated according to manufacturer specifications.

4.3 Ethical Considerations

As engineers, we are bound by the IEEE Code of Ethics to hold paramount the safety, health, and welfare of the public. Although combat robots operate against other robots in a controlled arena, there is an inherent risk of injury from high-speed mechanisms, high-current electrical systems, and lithium-polymer batteries.

- IEEE Code Section I.1 (Safety of the Public): We mitigate risks by implementing a physical kill switch, overcurrent protection on all motor channels, and a wireless heartbeat failsafe. All testing will follow ECE 445 lab safety protocols, including safety glasses and a controlled test enclosure.
- IEEE Code Section I.5 (Honest Representation): We will not falsely claim that our safety features prevent all accidents. The robot mitigates some hazards but does not eliminate the inherent risks of combat robotics. We will be honest about the system's capabilities and limitations.
- IEEE Code Section I.7 (Avoiding Conflicts of Interest): This project is academic with no commercial conflicts. All design decisions are made on engineering merit. We will credit all third-party designs, open-source code, and reference materials.
- ACM Code of Ethics Section 1.2 (Avoid Harm): The robot is a non-destructive control bot with no spinning weapons, inherently reducing the risk of projectile debris and catastrophic damage compared to spinner-class robots.

4.4 Safety Considerations and Mitigation

LiPo batteries can catch fire or explode if punctured, overcharged, over-discharged, or short-circuited. Mitigation measures include a firmware low-voltage cutoff at 3.3 V/cell, balance charging only in fireproof bags, physical protection of the battery within the chassis, hard disconnect via kill switch, and a 25 A fuse on the main positive rail. The system can draw up to 21 A from the battery. All high-current conductors will be a minimum of 16 AWG, and the main fuse coordinates with wiring limits. TVS diodes and flyback diodes suppress inductive transients. The PCB uses appropriate creepage/clearance per IPC-2221 for the 12 V rail. Moving parts can cause pinch and crush injuries. The arm links carry high forces. Mitigation: The robot will be operated only in designated test areas; hands will be kept clear of mechanisms during operation; and the kill switch will be used to disable all motion before handling. The robot uses no high-energy spinning weapons, significantly reducing projectile debris risk. During all testing in the ECE 445 lab, we will: wear safety glasses when the robot is powered, test within a controlled enclosure (acrylic box or arena walls), keep a fire extinguisher accessible when testing with LiPo batteries, never leave a charging LiPo unattended, and deactivate the kill switch before any physical contact with the robot.

4.5 Future Works

While the Scorpion-Lift BattleBot successfully met all baseline requirements, several areas were identified for further improvement and optimization in future iterations:

- **Center of Gravity and Weight Distribution:** A rearward center-of-gravity redesign would further improve the robot's inherent weight distribution and stability during opponent lifting maneuvers.
- **Enhanced PCB Design:** To provide a larger current margin for the actuators, an additional buck converter circuit should be added to the PCB specifically to support the 5 V power demand of the two lifting servos.
- **Closed-Loop Control:** Implementing closed-loop control and advanced sensing (such as utilizing the motor encoders) would provide more precise velocity and positional control of the drive system.
- **Control Interface:** We recommend leveling up the wireless control interface design to provide a more responsive and intuitive user experience for the operator.

References

[1] Battlebots Inc., “Competition Rules and Event History,” battlebots.com, 2024.

[2] R. Ciarcia, “Design Challenges in Small Combat Robots,” Make Magazine, vol. 78, pp. 42–49, 2023.

[3] IPC, “IPC-2221B: Generic Standard on Printed Board Design,” 2012.

[4] Pololu, “100:1 Metal Gearmotor 37Dx73L mm 12V with 64 CPR Encoder (Helical Pinion),” pololu.com, product #4755.

[5] DSSERVO, “DS3218 datasheet (Product datasheet, DS3218),” dsservo.com, 2018-07-30.

[6] Espressif, “ESP32-WROOM-32E Datasheet,” espressif.com, v1.2, 2023.

[7] Texas Instruments, “INA219 Bidirectional Current/Power Monitor Datasheet,” ti.com, SBOS448G, 2015.

[8] Pololu, “Pololu 30T Track Set - Black,” pololu.com, product #3033.

[9] Pololu, “50:1 Metal Gearmotor 37Dx70L mm 12V with 64 CPR Encoder (Helical Pinion),” pololu.com, product #4753.

Appendix A: Requirement and Verification Table

Subsystems	Requirements	Verification
Subsystem 1 Tracked Mobility	The drive system shall achieve a straight-line speed of at least **0.5 m/s** under full system load (all subsystems powered).	**Testing Distance:** 2.44 m **Time Taken:** Trial 1: 3.56 s Trial 2: 3.42 s Trial 3: 3.47 s Average: 3.48 s **Result:** Passed the test.
	The crowned-pulley tread geometry shall **prevent belt derailment** during full-differential zero-radius turns.	**Observation:** No tread derailment detected in the turning process. **Result:** Passed the test.
Subsystem 2 Dual Lifting Arms	Each lifting arm shall lift a **2 lb** test mass by at least **30 mm** within **3 seconds**.	**Observation:** Both arms lifted a 2 lb load by ≥ 30 mm **Time Taken:** 0.76 s. **Result:** Passed the test.

Subsystem 3 Scorpion Tail Stinger	The tail shall prevent the chassis from tipping backward when being lifted from the front by the opponent. The tipping angle when being lifted should be less than **45°**.	**Force Withstood:** 5.5 N **Maximum Chassis Pitch Angle:** 31° **Observation:** No full tip-over occurred during testing **Result:** Passed the test.
	The tail shall transition from stowed to bracing position in **≤1.0 s.**	**Tail Deployment Time:** 0.76 s **Result:** Passed the test.
Subsystem 4 Wireless Control	The wireless link (Wi-Fi) shall maintain a stable connection at a distance of up to **10 m** line-of-sight.	**Testing Distance:** 10.2 m **Observation:** Connection is stable. **Result:** Passed the test.

	The heartbeat failsafe shall disable all motor and actuator outputs within 500+300=**800 ms** of signal loss.	**Time Taken:** 580 ms **Result:** Passed the test.
Subsystem 5 Power and Safety	The battery power system shall supply sufficient current for all subsystems during peak operation **without shutdown or brownout**.	**Peak Battery Current:** 2601 mA **Observation:** No shutdown or brownout detected. **Result:** Passed the test.
	The battery shall supply sufficient current to run all subsystems for at least **2 minutes** continuously.	**Operating Time:** 2 minutes **Observation:** No communication loss or power interruption was observed. **Result:** Passed the test.